www.s2is.org
International Journal on Smart Sensing and Intelligent Systems
ISSN 1178-5608

NON-MINIMUM PHASE MODEL OF VERTICAL POSITION ELECTRO-HYDRAULIC CYLINDER FOR TRAJECTORY ZPETC

Norlela Ishak[1], Mazidah Tajjudin[1],Hashimah Ismail[2],Michael Patrick[1],Yahaya Md Sam[3],Ramli Adnan[1]

[1]Faculty of Electrical Engineering, Universiti Teknologi MARA (UiTM), 40450 Shah Alam, Selangor, Malaysia

[2]Faculty of Engineering, UNISEL, Selangor, Malaysia

[3]Faculty of Electrical Engineering, UTM Malaysia, Johor, Malaysia

Emails: norlelaishak@salam.uitm.edu.my, hashimah@unisel.edu.my, yahaya@utm.edu.my

Submitted: Apr. 16, 2012 Accepted: May 10, 2012 Published: June 1, 2012

Abstract— Hydraulic actuator has been widely used in industrial applications due to its fast response and capability of moving heavy load. The nonlinear properties of hydraulic cylinder had challenged researchers to design a suitable controller for position control, motion control and tracking control. Based on these problems, we had done a real-time digital tracking control studies on electro-hydraulic cylinder using trajectory zero phase error tracking control (ZPETC) without factorization of zeros polynomial algorithm. With the proposed strategy, the controller parameters are determined using comparing coefficients methods. The electro-hydraulic system mathematical model is approximated using system identification technique with non-minimum phase system being considered. The real-time experimental result will be compared with simulation result using a model from a real plant.

Keywords— Feedforward Control, ZPETC, System identification, pole placement, non-minimum phase

I. INTRODUCTION

Hydraulic actuator has been widely used in industrial equipments and processes due to its linear movements, fast response and accurate positioning of heavy load. This is principally due to its high-power density and system solution that it can provided [1,2]. The natural nonlinear property of hydraulic cylinder has challenged researchers in designing suitable controller for positioning control [3], motion control and tracking control [4]. With intention to improve the motion or tracking performance effectively, many researchers have used advanced control strategies to control hydraulic cylinder [5,6]. Classical feed-forward controller based on pole-zero cancellation for minimum phase system, makes the overall transfer function be unity thus perfect tracking control (PTC) is achieved [7]. Unfortunately, this controller cannot be implemented to non-minimum phase system as this would result an unstable tracking control. The zero-phase error- tracking control (ZPETC) was then proposed by Tomizuka [8] and has attracted attention many researchers as an effective and simple remedy to the problem due to unstable zeros. By eliminating phase error caused by non-cancelled zeros, ZPETC displays good tracking performance. The gain error, which cannot be eliminated by ZPETC becomes larger for fast tracking control and causes undesirable effect on the tracking performance. In resolving these problems, there has been many research works in this area [9-13].

Based on these scenarios, this paper discusses the implementation of real-time digital tracking control of electro-hydraulic cylinder using trajectory zero phase error tracking control without factorization of zeros polynomial where the controller parameters are determined using comparing coefficients method. Simulation and real-time experimental results will be compared and discusses on their tracking performances.

This paper was organized in the following manner: Section II describes ZPETC without factorization of zeros; Section III describes plant and model identification; Section IV describes controller design; Section V describes result and discussion; and Section VI is the conclusion.

II. ZPETC WITHOUT FACTORIZATION OF ZEROS

The tracking control system with two-degrees-of-freedom that is consisting of feedback and feedforward controllers is given in figure 1. In tracking control system without feedforward controller, the reference signal continuously varying and mixed with the closed-loop system dynamics, which make function of feedback controller is regulation against disturbance inputs. The feedforward controller is required such that the reference signal can be pre-shaped by the feedforward controller, so that more emphasis to the frequency components that were not sufficiently handled by the feedback system can be provided [6].

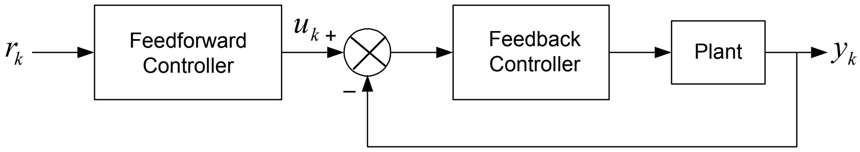

Figure 1. Two-degree-of-freedom controller

Referring to figure 1, the closed-loop transfer function of the system (without feedforward control) can be represented by the following discrete time model:

$$G_{cl}(z^{-1}) = \frac{z^{-d} B_c(z^{-1})}{A_c(z^{-1})} \tag{1}$$

where

$$A_c = 1 + \alpha_1 z^{-1} + \alpha_2 z^{-2} + \dots\dots\dots + \alpha_{n_a} z^{-na}$$

$$B_c(z^{-1}) = \beta_o + \beta_1 z^{-1} + \beta_2 z^{-2} + \dots + \beta_{n_a} z^{-nb}$$

d = time delay

The function B_c (z^{-1}) can be factorized into minimum phase and non-minimum phase factors:

$$B_c(z^{-1}) = B_c^{+}(z^{-1}) B_c^{-}(z^{-1}) \tag{2}$$

where $B_c^{+}(z^{-1})$ denotes the minimum phase factor and $B_c^{-}(z^{-1})$ denotes the non-minimum phase factor. The conventional ZPETC reported in the literature [14] can be divided into three blocks as shown in figure 2. The block diagram of feedforward ZPETC consists of the gain compensation filter, phase compensation filter and stable inverse. Figure 3 shows the structure of the ZPETC feedforward controller without zeros factorization. The block diagram of feedforward ZPETC without factorization of zeros consists of the gain compensation filter, phase compensation filter and closed-loop transfer function denominator.

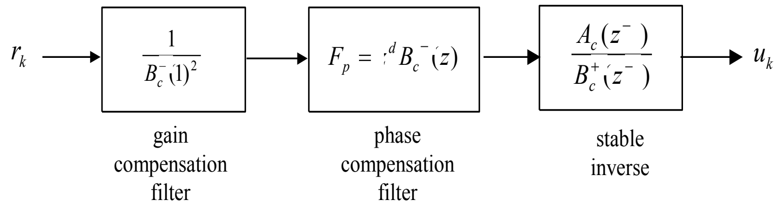

Figure 2. Conventional ZPETC structure block diagram

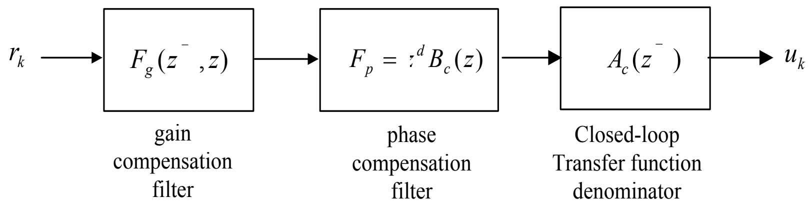

Figure 3. ZPETC without factorization of zeros structure block diagram

Similar to all others ZPETC, the design mainly focused on the selection of appropriate gains compensation filter to ensure the overall gain is unity within the frequency spectrum of reference trajectory. To ensure the gain compensation filter, F_g does not introduces any phase error, the same approach done by [15-16] will be followed. The FIR symmetric filter was used. The filter is represented by equation

$$F_g(z,z^{-1}) = \sum_{k=0}^{n_\alpha} \alpha_k (z^k + z^{-k}) \tag{3}$$

where n_α is the order of the filter. A suitable cost function to represent the error between the desired and actual frequency response is given by Eq. (4).

$$J(\alpha_k) = \left\| 1 - B_c(z^{-1}) B_c(z) \sum_{k=0}^{n_\alpha} \alpha_k (z^k + z^{-k}) \right\|_{l_2} \tag{4}$$

The design objective here is to find a set of α_k such that the cost function given by Eq. (4) is minimized. For finite α_k, Eq.(4) cannot be made zero for all frequencies. By minimizing the cost function of Eq. (4),

$$B_c(z^{-1}) B_c(z) \sum_{k=0}^{n_\alpha} \alpha_k (z^k + z^{-k}) = \tag{5}$$

The optimal set of α_k can be obtained by expanding Eq. (5) to polynomial of positive and negative power of z, and then compare the coefficients of the same power.

III. PLANT AND MODEL IDENTIFICATION

A. Plant

The experimental equipment that used in these real-time studies is an electro-hydraulic system that is shown in figure 4. The hydraulic cylinder was held in vertical position. This is a very challenging problem as effect of gravity is trivial. The electro-hydraulic system consists of single-ended cylinder type of actuator. The bidirectional cylinder has 150 mm stroke length; 40 mm bore size and 25 mm rod size. The wire displacement sensor is mounted at the top of cylinder rod. The pressurized fluid flow is control by electronic control valve. The interfacing between the computer and plant was done using Matlab Real-Time Workshop via Advantech PCI-1716 interface card.

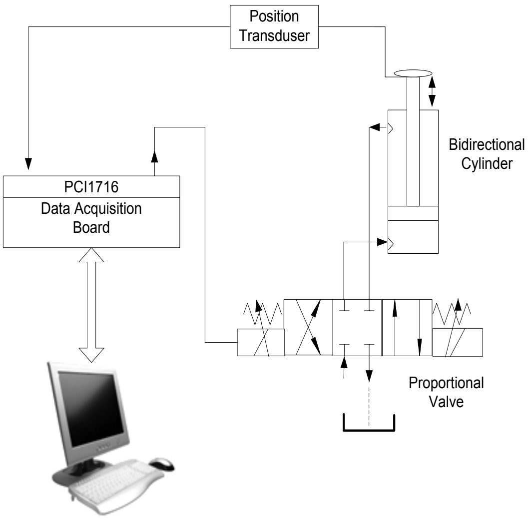

Figure 4. Experimental setup for electro-hydraulic system

B. Model Identification

The plant model that used in these studies was obtained through open-loop experiment on the Electro-hydraulic system of figure 4. The open-loop transfer function of the plant was approximated using Matlab System Identification Toolbox. The signal given in figure 5 was used as an input signal to the plant for model identification. The signal was generated using three different frequencies based on Eq. (6) and represented by Eq. (7).

$$u(k) = \sum_{i=1}^{p} a_i \cos \omega_i s k \tag{6}$$

$$V_{in}(k) = 2\ Cos\ 0.3\ t_s k + 2\ Cos\ 4\ t_s k + Cos\ 6\ t_s k \tag{7}$$

where a_i is the amplitude, ω_i is the frequency (rad/sec), t_s is the sampling time (sec) and k is integer.

From Eq. (7), when using three different frequencies for input signal, the model that can be obtained is limited to second and third order only. Higher-orders model may produce unstable output. In these studies, the third-order ARX331 model with input-output signals sampled at 50ms was selected to represent the nearest model of true plant.

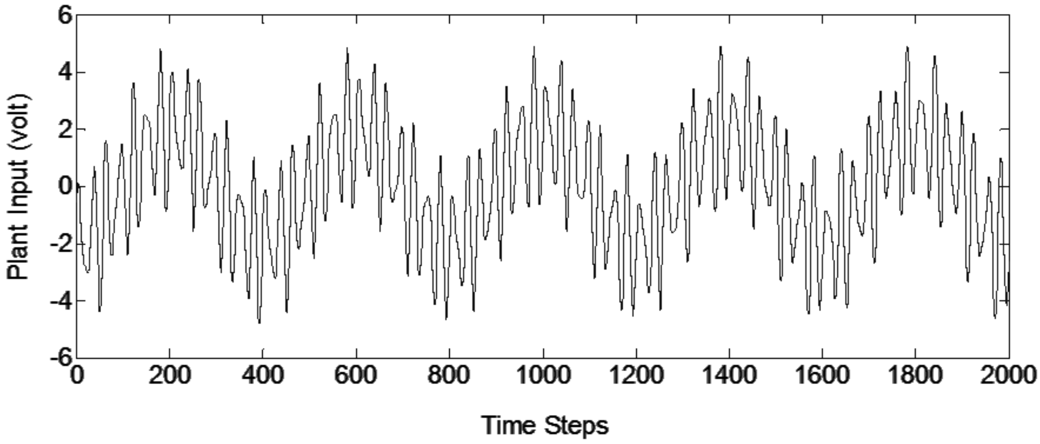

Figure 5. Input signals for model identification

The output signal of the plant obtained using the input signal of figure 5 and sampled at 50 ms, is given in figure 6. The input and output signals of Figure 5 and Figure 6 were divided into two parts, i.e. (500-1000) samples and (1001-1500) samples. The first part of the input – output signals were used to obtain the plant model and the second part of the input-output signals were used to validate the obtained model.

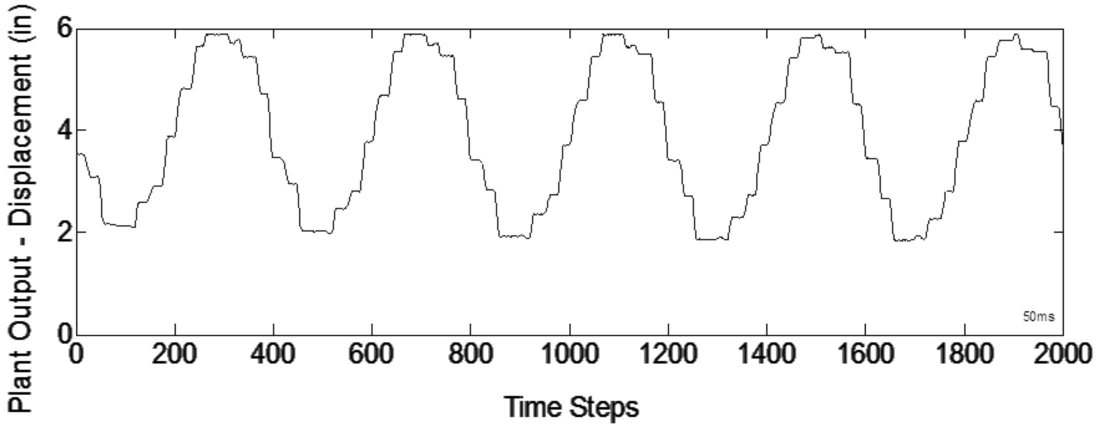

Figure 6. Output signal of the plant using 50 ms sampling time

Using Matlab System Identification Toolbox, the first part of the input-output signal produces a plant model, ARX331 in the form of discrete-time open-loop transfer function as follows:

$$\frac{B_o(z^{-})}{A_o(z^{-})} = \frac{0.0087z^{-} +).0037z^{-} -).0088z^{-}}{1 - .5800z^{-} +).3938z^{-} +).1861z^{-}} \quad (8)$$

From Eq. (8), its can be simplified as

$$\frac{B_o(z^{-})}{A_o(z^{-})} = \frac{).0087z^{-}(1 +).4232z^{-} - .0148z^{-})}{1 - .5800z^{-} +).3938z^{-} -).1861z^{-}} \quad (9)$$

From Eq. (9), the zeros polynomial is given by

$$B_c(z^{-}) = \; +).4232z^{-} - .0148z^{-} \quad (10)$$

$$B_c(z) = \; +).4232z - .0148z^2$$

When Eq. (10) is factorized, the locations of zero are at z = 0.8178 and z = -1.2410. This means that the model obtained is a non-minimum phase model with a zero situated outside the unity circle. A non-minimum phase model can be obtained using small sampling time whereas minimum phase model can be obtained using larger values of sampling time [17]. The pole-zero plot of Eq. (10) is given in figure 7.

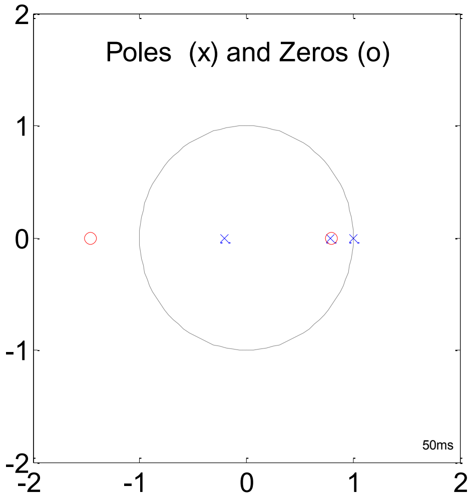

Figure 7. Pole-zero plot of Eq. (10)

The second part of input-output signals were used to validate the obtained model of Eq. (8). The second part of the input signal is used as an input to the model and the output from the model was compared with the second part of the output signal. The result can be seen from figure 8. Using model selection criterions, the following information were obtained:

Best Fit :	89 %
Loss Function :	3.292 e^{-005}
Akaike's Final Prediction Error, FPE:	3.371 e^{-005}

Based on the smallest values criteria of FPE and Best Fit of 89 %, this model can be accepted.

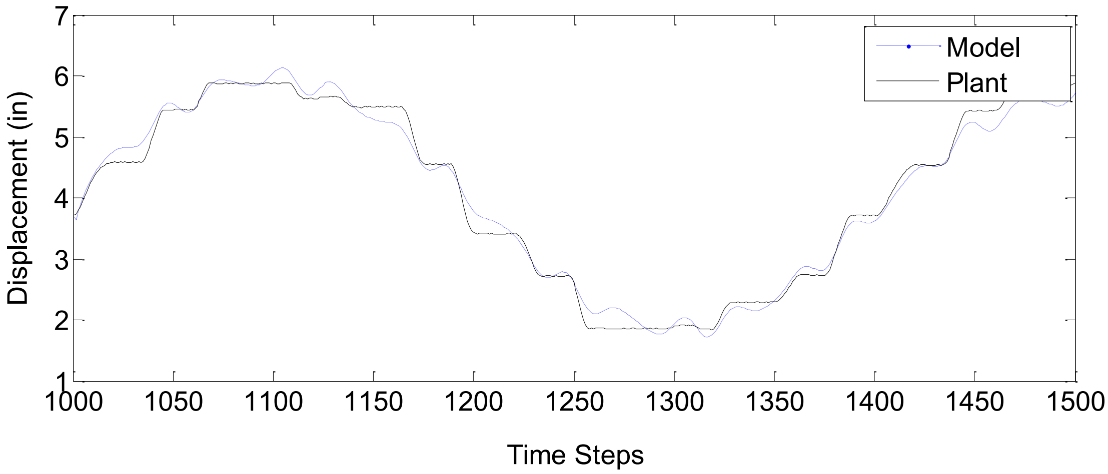

Figure 8. Comparison between the model and plant output signal

IV. CONTROLLER DESIGN

A. Trajectory ZPETC Scheme

This section presents the proposed trajectory zero phase error tracking control (ZPETC) without factorization of zeros polynomial as given in figure 9 where the controller parameters are determined using comparing coefficients method.

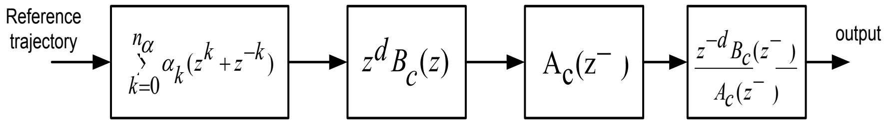

Figure 9. Trajectory ZPETC structure

The design objective here is to find an optimal set of α_k by minimizing the cost function of Eq. (5). The optimal set of α_k can be obtained by expanding Eq. (5) to polynomial of positive and negative power of z, and then compare the coefficients of the same power. From Eq. (9) and (10), the optimal set of α_k for 5th order gain compensation filter is obtained as follows:

$$\left[\left(1+0.4232z^{-1}-1.0148z^{-2}\right)\left(1+0.4232z^{1}-1.0148z^{-2}\right)\right] . \sum_{k=0}^{n_\alpha} \alpha_k\left(z^k+z^{-k}\right) = 1$$

and

$$\left[\begin{array}{l} .2089 - 0.1971(z+z^{-1}) \\ - .0148(z^2+z^{-2}) \end{array}\right]\left[\begin{array}{l} 2\alpha_0 + \alpha_1(z+z^{-1}) + \alpha_2(z^2+z^{-2}) + \alpha_3(z^3+z^{-3}) \\ + \alpha_4(z^4+z^{-4}) + \alpha_5(z^5+z^{-5}) \end{array}\right] = \qquad (11)$$

By expanding Eq. (11) to polynomial of positive and negative power of z and then compare the coefficients of the same power, the following equation is obtained:

$$\begin{bmatrix} 2.2089 & -0.0125 & -2.0296 & 0 & 0 & 0 \\ -0.0063 & 1.1941 & -0.0063 & -1.0148 & 0 & 0 \\ -1.0148 & -0.0063 & 2.2089 & -0.0063 & -1.0148 & 0 \\ 0 & -1.0148 & -0.0063 & 2.2089 & -0.0063 & -1.0148 \\ 0 & 0 & -1.0148 & -0.0063 & 2.2089 & -0.0063 \\ 0 & 0 & 0 & -1.0148 & -0.0063 & 2.2089 \end{bmatrix} \begin{bmatrix} 2\alpha_0 \\ \alpha_1 \\ \alpha_2 \\ \alpha_3 \\ \alpha_3 \\ \alpha_5 \end{bmatrix} = \begin{bmatrix} 1 \\ 0 \\ 0 \\ 0 \\ 0 \\ 0 \end{bmatrix} \quad (12)$$

Solving Eq.(12), the optimal set of α_k is obtained. In these studies, we consider the order of $F_g\ (z^{-1}, z)$ is n_α = 10, 20 and 30. The optimal α_k obtained by minimizing the cost function is given in Table I. When the filter order is increase to 20th and 30th order, using the same technique, the obtained optimal set of α_k is given in Table II and Table III. The results show that the values obtained are almost converging to zero, as the filter order increasing, as shown in figure 10.

Table I:
Optimal α_k for 10th order gain compensation filter of Eq. (8)

k	0	1	2	3	4	5	6	7	8	9	10
α_k	0.7159	0.3738	0.4679	0.3064	0.3139	0.2258	0.2061	0.1479	0.1231	0.0743	0.0553

Table II:
Optimal α_k for 20th order gain compensation filter of Eq. (8)

k	0	1	2	3	4	5	6	7	8	9	10
α_k	0.3785	0.4274	0.5151	0.3629	0.3691	0.2896	0.2716	0.2243	0.2020	0.1706	0.1501
k	11	12	13	14	15	16	17	18	19	20	
α_k	0.1275	0.1102	0.0930	0.0789	0.0651	0.0536	0.0416	0.0326	0.0207	0.0147	

Table III:
Optimal α_k for 30th order gain compensation filter of Eq. (8)

k	0	1	2	3	4	5	6	7	8	9	10
α_k	0.3834	0.4255	0.5208	0.3621	0.3724	0.2901	0.2743	0.2261	0.2051	0.1738	0.1546
k	11	12	13	14	15	16	17	18	19	20	21
α_k	0.1328	0.1169	0.1011	0.0884	0.0766	0.0668	0.0579	0.0502	0.0434	0.0375	0.0322
k	22	23	24	25	26	27	28	29	30		
α_k	0.0275	0.0234	0.0197	0.0163	0.0134	0.0104	0.0081	0.0052	0.0037		

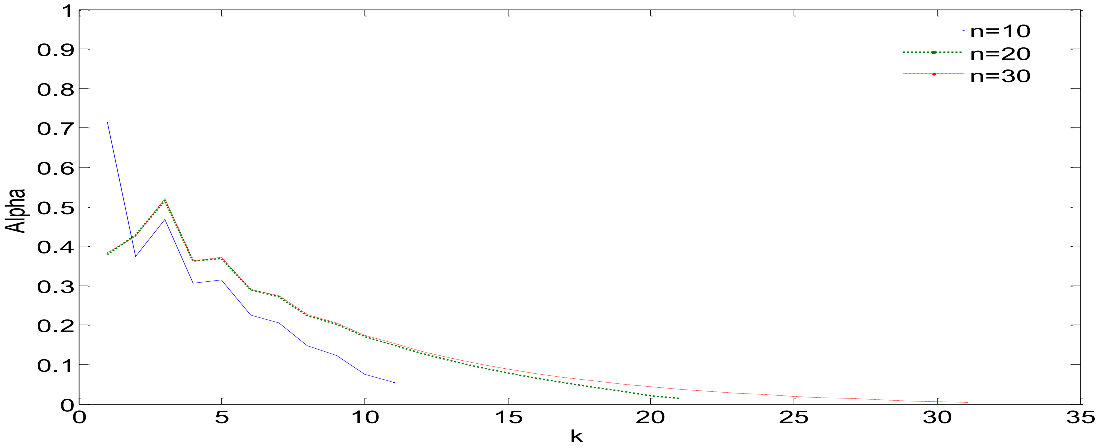

Figure 10. Optimal α_k of order filter

B. Simulation Studies

The implementation of simulation studies that based on figure 9 can be simplified to the control structure of figure 11 due to the effect of poles cancellation to the trajectory ZPETC structure. From this figure, we can see that the implementation of tracking control by simulation does not required the whole plant model transfer function. What is needed only the zero polynomial equation of the plant model.

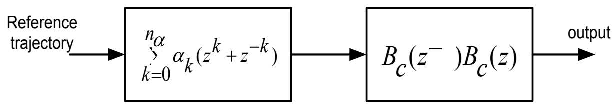

Figure 11. Tracking control structure for simulation studies.

C. Real-Time Studies

For real-time studies, we proposed the control structure given in figure 12. This control structure consists of two parts, which are feedforward control and feedback control. For feedforward control, we used the trajectory-ZPETC structure. For feedback control, we used the pole-placement method [18]. This method enable all poles of the closed –loop to be placed at desired location and providing satisfactory and stable output performance.

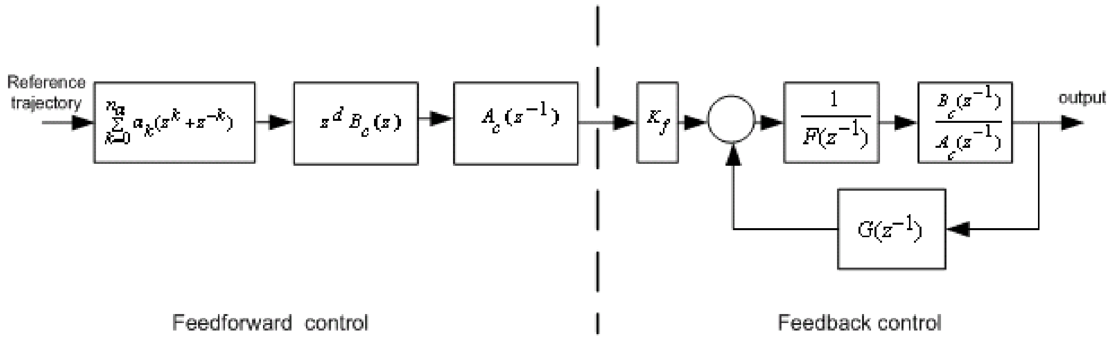

Figure 12. Tracking structure for real-time studies

D. Feedback Control System

The feedback control system for the proposed trajectory ZPETC system is given in figure 13. The controller was designed using pole-placement method.

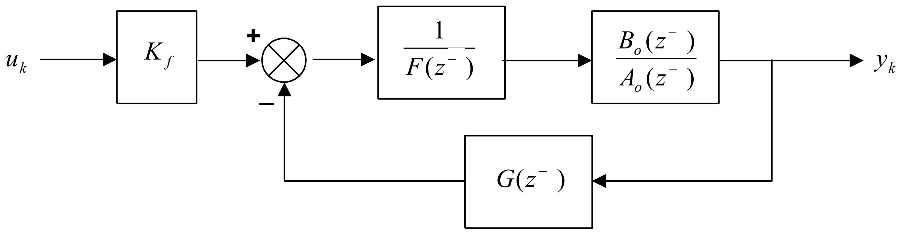

Figure 13. Feedback controller using pole-placement method.

This method enables all poles of the closed-loop to be placed at desired location and providing satisfactory and stable output performance. All controller parameters were obtained by solving the following Diophantine equation to solve for $F\ (z^{-1})$ and $G\ (z^{-1})$.

The closed-loop transfer function of the system is given by:

$$\frac{Y(z^{-})}{U(z^{-})} = \frac{K_f B_O(z^{-})}{A_O(z^{-})F(z^{-}) + B_O(z^{-})G(z^{-})} \qquad (13)$$

where

$$A_o(z^{-1}) = 1 + a_1 z^{-1} + a_2 z^{-2} + a_3 z^{-3} + \cdots + a_n z^{-}$$
$$B_o(z^{-1}) = b_1 z^{-1} + b_2 z^{-2} + b_3 z^{-3} + \cdots + b_m z^{-}$$
$$F(z^{-}) = + f_1 z^{-} + f_2 z^{-} + f_3 z^{-} + \cdots + f_m z^{-m-}$$
$$G(z^{-}) = g_0 + g_1 z^{-} + g_2 z^{-} + g_3 z^{-} + \cdots + g_{n-} z^{-n-}$$

Using Diophantine equation to solve for $F(z^{-})$ and $G(z^{-})$,

$$A_o(z^{-})F(z^{-}) + B_o(z^{-})G(z^{-}) = T(z^{-}) \tag{14}$$

with $T(z^{-}) = + t_1 z^{-}$ and t_1 is the location of a pole in a unit circle. The range of t_1 is $0 < t_1 <$. For slow response, t_1 is set large and for fast response, t_1 is set small. The forward gain $K_f = \dfrac{Sum(T)}{Sum(B_o)}$.

In this paper, we used $t_1 = 0.8$ since the tracking required slow response. Attempts have been made to use small values of t_1, but the responses are very fast and producing large tracking errors. Using developed Visual C++ console programming and Matlab/Simulink, the following parameters were computed:

$$T = - 0.82z^{-}$$
$$K_f = 0$$
$$F(z^{-}) = + 0.2189z^{-} - 0.2165z^{-}$$
$$G(z^{-}) = 2.1614 - .9397z^{-} - .5606z^{-}$$

V. RESULTS AND DISCUSSION

In this section, the simulation and real-time results were analyzed to show the effectiveness of the designed controller. The simulation and real-time result of using controller parameters are given in Table I, II and III and applied to plant model which resulting RMSE that given in Table IV.

Table IV:
RMSE performance (mm)

	Simulation			Real-Time		
n_α	10	20	30	10	20	30
RMSE	11.242	2.1692	0.7772	11.460	2.4435	1.3665

The tracking performances in terms of root mean squared error (RMSE) for all the simulated and real-time results are summarized in Table IV. The results show the 10th, 20th and 30th order filter tracking performances. It can be observed that the tracking error has been greatly reduced when the filter order was increased. As we can observe from the simulated results of Table IV, by introducing larger filter order to the system, the performance between 10th and 20th order filter has improved by 80%. For the real-time result, by introducing larger order filter, the performance between 10th and 20th has improved by 78%. However, the result between the simulated and real-time does not provide similar performance due to plant-model mismatch.

Figure 14, shows the frequency response for the overall system. The frequency response can be improved if the order of $F_g\ (z^{-1}, z)$ is increased. Based on figure 14, it can be observed that by using 10th order filter, it will not able to produce a gain that near to unity. The gain is almost flat at unity when a higher order filter is used.

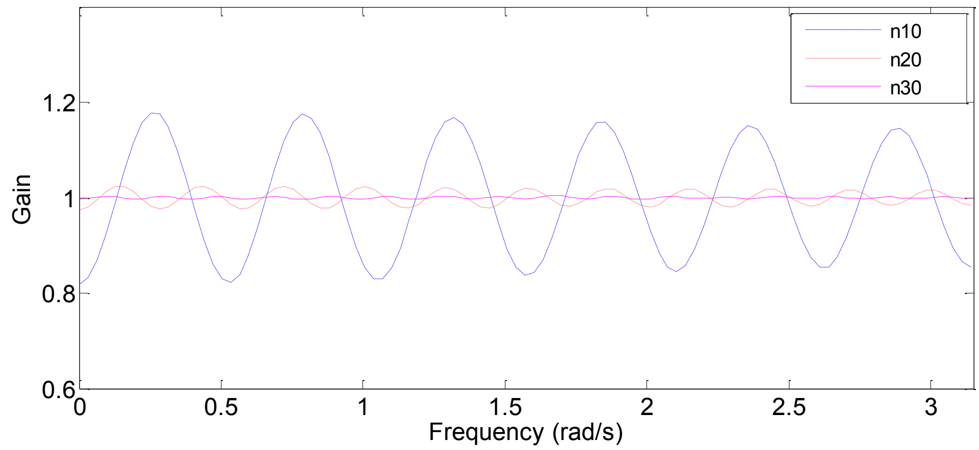

Figure 14. Frequency response of 10th, 20th and 30th order ZPETC

Figure 15(a) and (b) show poor tracking performance when 10th order filter was used. The result is already being expected due to the frequency response given in figure 14. The tracking RMSE error is 11.460 mm. It is clear that using 10th order filter will not produce satisfactory tracking performance. Figure 16(a) and (b) resulting tracking RMSE error of 2.4435 mm. The tracking error is much smaller as compared to figure 15(a,b). This can be observed from frequency response given in figure 14, when 20th order filter was used. The unity gain line obtained is much better compared to 10th order filter.Figure 17(a) and (b) resulting tracking RMSE error of 1.3665 mm, which is much better that the one given in figure 16(a,b). In fact, the overlapping of reference and output signals cannot be seen. The RMSE tracking error can be reduced further by increasing the order filter. Higher order filter can approximate the overall transfer function of the system very close to unity for all frequencies effectively. This is explained by the frequency response of figure 14.

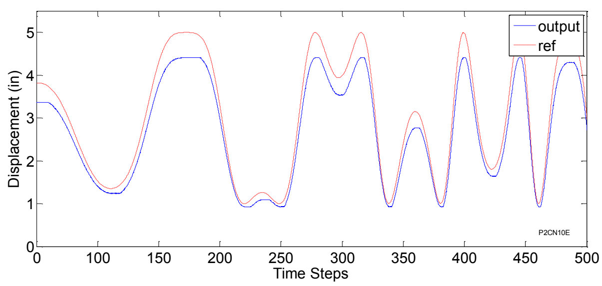

Figure 15(a). Experimental result using 10th order ZPETC

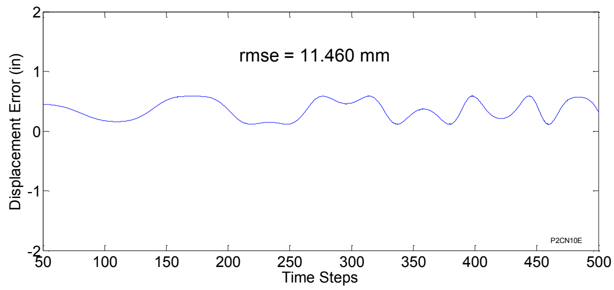

Figure 15(b). Tracking Error using 10thorder ZPETC

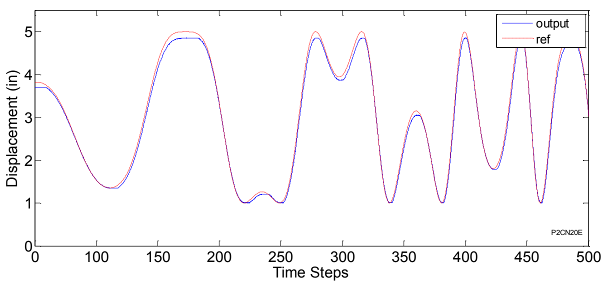

Figure 16(a). Experimental result using 20th order ZPETC

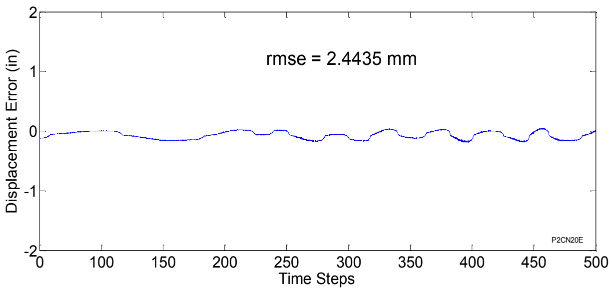

Figure 16(b). Tracking Error using 20thorder ZPETC

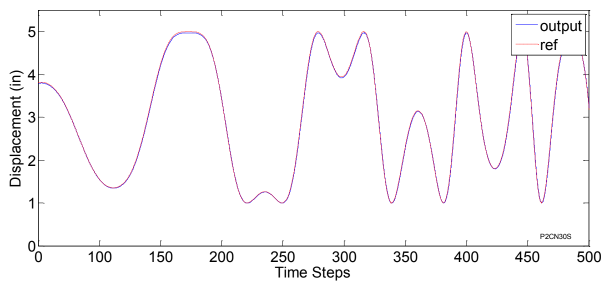

Figure 17(a). Experimental result using 30th order ZPETC

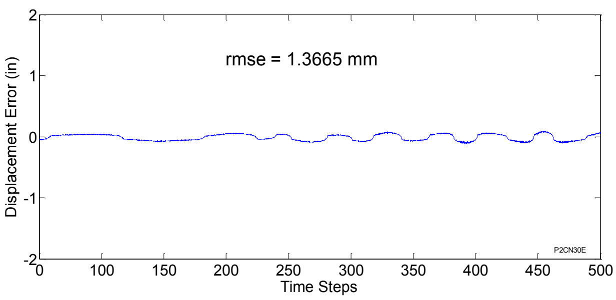

Figure 17(b). Tracking Error using 30thorder ZPETC

VI. CONCLUSIONS

A controller design using trajectory ZPETC without factorization of zeros polynomial has been presented. The proposed feedforward controller design has been successfully tested by simulation and validated by real-time digital control of electro-hydraulic cylinder. Simulation and experimental results show good tracking performances when higher order filter was used in the design. A much smaller tracking error cannot be achieved due to plant-model mismatch and electronic valve open-close capability.

ACKNOWLEDGMENT

The authors would like to thank and acknowledge the FRGS-RMI-UiTM (600-RMI/ST/FRGS 5/3/Fst(85/2010) for financial support of this research

REFERENCES

[1] Shao, J., Wang, Z., Lin, J. and Han, G., “Model Identification and Control of Electro-Hydraulic Position Servo System”, Proc. *Int.Conf. On Intelligent Human-Machine Systems and Cybernetics* (IHMSC 09), Hangzhou, Zhejiang, China, 2009, pp. 210-213

[2] Chen, H.M., Renn, J.C. and Su, J.P., “Sliding Mode Control with Varying Boundary Layers for an Electro-Hydraulic Position Servo System”, Int. J. of Advanced Manufacturing Technology, vol. 26, 2005, pp. 117–123

[3] Kaddissi, C., Kenne, J-P. And Saad, M., “Identification and Real- Time Control of an Electrohydraulic Servo System Based on Nonlinear Backstepping”, IEEE/ASME J. Mechatronics, vol. 12, no. 1, 2007, pp. 12–22

[4] Zhu, W.H. and Piedboeuf, J.C., “Adaptive Output Force Tracking Control of Hydraulic Cylinder with Application to Robot Manipulators”, ASME J. of Dyn. Syst., Meas., and Control, vol. 127, 2005, pp. 206–217

[5] Eryilmaz, B. and Wilson, B.H., “Improved Tracking Control of Hydraulic Systems”, ASME J. of Dyn. Syst., Meas., and Control, vol. 123, 2001, pp. 457–462

[6] Tsao, T.C. and Tomizuka, M., “Robust Adaptive and Repetitive Digital Tracking Control and Application to a Hydraulic Servo for Noncircular Machining”, ASME J. of Dyn. Syst., Meas., and Control, vol. 116, 1994, pp. 24–32

[7] Liu, Q., and Feng, S-T., "Tracking Control of Nonminimal Phase System Without Using Preview Information of the Desired Output", Proc. *6th Int. Conf. On Machine* Learning Cybernetics, Hong Kong, vol. 1, 2007, pp. 588-591

[8] Tomizuka, M., "Zero Phase Error Tracking Algorithm for Digital Control," ASME J. of Dyn. Syst., Meas., and Control, vol. 109, 1987, pp. 65–68

[9] Haack, B. and Tomizuka, M., "The Effect of Adding Zeroes to Feedforward Controllers," ASME J. of Dyn. Syst., Meas., and Control, vol. 113, 1991, pp. 6–10

[10] Torfs, D., De Schutter, J. and Swevers, J., "Extended Bandwidth Zero Phase Error Tracking Control of Non-minimum Phase Systems," ASME J. of Dyn. Syst., Meas., and Control, vol. 114, 1992, pp.347–351

[11] Xia, J.Z. and Menq, C.H., "Precision Tracking Control of Non-minimum Phase Systems with Zero Phase Error," Int. J. Control, vol. 61, no. 4, 1995, pp. 791-807

[12] Yamada, M., Funahashi, Y. and Riadh, Z., "Generalized Optimal Zero Phase Error Tracking Controller Design," ASME J. of Dyn. Syst., Meas., and Control, vol. 121, 1999, pp. 165–170

[13] Park, H.S., Chang, P.H. and Lee, D.Y., "Concurrent Design of Continuous Zero Phase Error Tracking Controller and Sinusoidal Trajectory for Improved Tracking Control," ASME J. of Dyn. Syst., Meas., and Control, vol.123, 2001, pp. 127–129

[14] Tomizuka, M., "*On the Design of Digital Tracking Controllers*," ASME J. of Dyn. Syst., Meas., and Control, vol. 115,1993, pp.412–418

[15] Yeh, S.S. and Hsu, P.L., "An Optimal and Adaptive Design of the Feedforward Motion Controller", IEEE/ASME J. Mechatronics, vol. 4, no. 4, 1999, pp. 428–439

[16] Mustafa, M.M., "Trajectory-Adaptive Digital Tracking Controllers for Non-minimum Phase Systems Without Factorisation of Zeros", IEE Proc. Control Theory Appl., vol. 149, no. 2, 2002, pp. 157–162

[17] Astrom, K.J. and Wittenmark, B., *Computer-Controlled Systems:Theory and Design*, 3rd ed., Prentice Hall, Englewood Cliffs, N.J.,1997.

[18] Landau, I.D., *System Identification and Control Design Using P.I.M.+Software*, Prentice Hall, Englewood Cliffs, N.J., 1990